Biochimica et Biophysica Acta 1788 (2009) 390–401

Contents lists available at ScienceDirect

Biochimica et Biophysica Acta

journal homepage: www.elsevier.com/locate/bbamem

Effects of temperature and pressure on the lateral organization of model membranes with functionally reconstituted multidrug transporter LmrA

Nagarajan Periasamy [a], Holger Teichert [b], Katrin Weise [a], Rudi F. Vogel [b], Roland Winter [a,*]

[a] Dortmund University of Technology, Physical Chemistry I — Biophysical Chemistry, D-44227 Dortmund, Germany
[b] Technische Universität München, Lehrstuhl für Technische Mikrobiologie Weihenstephan, Weihenstephaner Steig 16, D-85350 Freising, Germany

ARTICLE INFO

Article history:
Received 3 June 2008
Received in revised form 19 September 2008
Accepted 24 September 2008
Available online 17 October 2008

Keywords:
LmrA
High hydrostatic pressure
Fluorescence spectroscopy
Phospholipid
Lipid phase transition
Raft mixture

ABSTRACT

To contribute to the understanding of membrane protein function upon application of pressure, we investigated the influence of hydrostatic pressure on the conformational order and phase behavior of the multidrug transporter LmrA in biomembrane systems. To this end, the membrane protein was reconstituted into various lipid bilayer systems of different chain length, conformation, phase state and heterogeneity, including raft model mixtures as well as some natural lipid extracts. In the first step, we determined the temperature stability of the protein itself and verified its reconstitution into the lipid bilayer systems using CD spectroscopic and AFM measurements, respectively. Then, to yield information on the temperature and pressure dependent conformation and phase state of the lipid bilayer systems, generalized polarization values by the Laurdan fluorescence technique were determined, which report on the conformation and phase state of the lipid bilayer system. The temperature-dependent measurements were carried out in the temperature range 5–70 °C, and the pressure dependent measurements were performed in the range 1–200 MPa. The data show that the effect of the LmrA reconstitution on the conformation and phase state of the lipid matrix depends on the fluidity and hydrophobic matching conditions of the lipid system. The effect is most pronounced for fluid DMPC and DMPC with low cholesterol levels, but minor for longer-chain fluid phospholipids such as DOPC and model raft mixtures such as DOPC/DPPC/cholesterol. The latter have the additional advantage of using lipid sorting to avoid substantial hydrophobic mismatch. Notably, the most drastic effect was observed for the neutral/glycolipid natural lipid mixture. In this case, the impact of LmrA incorporation on the increase of the conformational order of the lipid membrane was most pronounced. As a consequence, the membrane reaches a mechanical stability which makes it very insensitive to application of pressures as high as 200 MPa. The results are correlated with the functional properties of LmrA in these various lipid environments and upon application of high hydrostatic pressure and are discussed in the context of other work on pressure effects on membrane protein systems.

1. Introduction

Membrane protein function is generally influenced by the molecular composition and phase state of the host lipid bilayer and interaction with lipids, specifically phospholipids and cholesterol [1–4]. Saturated phospholipids often exhibit two thermotropic lamellar phase transitions, a gel-to-gel ($L_{\beta'}/P_{\beta'}$) pre-transition and a gel-to-liquid-crystalline ($P_{\beta'}/L_{\alpha}$) main transition at a higher temperature T_m [5]. In the fluid-like L_{α} phase, the hydrocarbon chains of the lipid bilayers are conformationally disordered, whereas in the gel phases the chains are more extended and ordered. Changes in environmental conditions, such as temperature and pressure [6–8], produce alterations in the lateral structure and phase behavior of the membrane, which can lead to conformational changes of membrane associated proteins and their distribution in the host membrane. As a consequence, their functional properties may be altered.

In physico-chemical and biochemical studies, the interest in pressure as a variable to also study lipid mesophase transitions, membrane fusion, protein unfolding and refolding as well as protein aggregation and fibrillation has been growing over the last years [9–15]. Very little is known about pressure effects on membrane proteins. However, some groups have described very interesting pressure-induced effects on enzymatic catalysis by membrane proteins [16–22]. High hydrostatic pressure has also started to be exploited in diverse areas of biotechnology, including the ability to modify the catalytic specificity of enzymes [23].

In this work, we examined the influence of the lipid matrix and of hydrostatic pressure on lipid–protein interactions in different membrane systems using the multidrug resistance protein LmrA. LmrA was

Abbreviations: DMPC, 1,2-dimyristoyl-*sn*-glycero-3-phosphatidylcholine; DOPC, 1,2-dioleoyl-*sn*-glycero-3-phosphatidylcholine; Chol, cholesterol; SM, sphingomyelin; PC, phosphatidylcholine; Laurdan, 6-dodecanoyl-2-dimethylamino-napthalene; *GP*, generalized polarization; LAB, lactic acid bacteria; MDR, multidrug resistance transporters; DDM, dodecyl maltoside

* Corresponding author. Tel.: +49 231 755 3900; fax: +49 231 755 3901.
E-mail address: roland.winter@uni-dortmund.de (R. Winter).

0005-2736/$ – see front matter © 2008 Elsevier B.V. All rights reserved.
doi:10.1016/j.bbamem.2008.09.017

expressed in *Lactococcus lactis* and functionally reconstituted in different model membrane systems. These systems are composed of DMPC, DOPC, DMPC+10 mol% cholesterol (Chol), and the model raft mixture DOPC:DPPC:Chol (1:2:1). In addition, particular natural membrane lipids extracted from *Lactobacillus plantarum* were used. Circular dichroism (CD) spectroscopy and atomic force microscopy (AFM) were applied to characterize the secondary structure of LmrA and to control the lipid reconstitution into the various lipid bilayer systems. Information on the lipids' lateral membrane organization and the temperature and pressure dependent phase behavior of the membrane systems was examined by Laurdan fluorescence spectroscopy.

In the lactic acid bacterium (LAB) *L. lactis*, several multidrug-resistance transporters (MDR) were found to confer resistance to cationic lipophilic cytotoxic compounds [24], which includes LmrP as a representative of the secondary MDR transporters [25], and LmrA as a representative of the ABC transporter family [26], which can also be found in *L. plantarum* and in the strain TMW 1.460. In another LAB *Lactobacillus brevis*, a homolog of LmrA was found that confers resistance to hop [27]. This LmrA homolog is encoded by the gene called HorA. Protein LmrA and HorA contribute to the intrinsic drug resistance of the organisms in which they are expressed. LmrA causes antibiotic resistance by expelling amphiphilic compounds from the inner leaflet of the cytoplasmic membrane [28,29]. Unlike other bacterial multidrug-resistance proteins, LmrA is the first ABC-transporter found in bacteria to confer multidrug resistance [30]. It is a 590 amino acid protein with an N-terminal hydrophobic domain, consisting of six transmembrane helices, followed by a C-terminal hydrophilic domain, containing the ATP-nucleotide binding site. Although its topology in the lipid membrane had been predicted from its primary structure and many models were proposed, a well defined tertiary structure is not known. LmrA has the broadest substrate specificity reported for MDRs. The human multidrug-resistance plasma membrane glycoprotein (P-glycoprotein or P-gp), encoded by the *MDR1* gene, is also an ABC transporter. The most commonly accepted topology model suggests that these MDR proteins are constituted of two homologous halves composed of an ATP-binding domain and a membrane-embedded domain [31]. LmrA has about 50% similarity with each of the P-glycoprotein halves and functions as a homodimer [28]. Hence functional crosstalk between two LmrA monomers in a lipid matrix is essential for its activity [32]. LmrA exhibits specificity for phospholipid head groups and may be involved in the lipid sorting in *L. lactis* [26]. Bacterial LmrA and human P-glycoprotein are functionally interchangeable and this type of MDR nature is probably conserved from bacteria to man [28]. The mechanism of extrusion of cytotoxic compounds by LmrA has been studied in whole cells, isolated membrane vesicles and proteoliposomes. These studies revealed that the lipophilic substrates intercalate rapidly in the outer leaflet of the membrane. Subsequently, the substrate flips over slowly to the inner leaflet from where it is picked up by LmrA and extruded in an ATP-dependent process to the external medium [29].

The main purpose of our work was to examine the influence of various lipid matrices and of hydrostatic pressure on lipid–protein interactions using this multidrug resistance protein LmrA as a valuable model system. The results are then compared with the function of the enzyme upon pressurization and are discussed in the context of pressure studies on other membrane protein systems.

2. Materials and methods

2.1. Materials

1,2-Dioleoyl-*sn*-glycero-3-phosphocholine (DOPC), 1,2-dipalmitoyl-*sn*-glycero-3-phosphocholine (DPPC), and 1,2-dimyristoyl-*sn*-glycero-3-phosphocholine (DMPC) were purchased from Avanti Polar lipids (Alabaster, AL), cholesterol (Chol) from Sigma-Aldrich. Laurdan (6-dodecanoyl-2-dimethyl aminonapthalene) was obtained from Molecular Probes Inc. (Eugene, OR), dodecyl maltoside (DDM) from GERBU Biochemicals GmbH, Germany, and biobeads SM-2 adsorbent from Bio-Rad. All other materials were reagent grade and purchased from commercial sources. All chemicals were used without further purification. LmrA protein was expressed and purified by Holger Teichert from the Technische Universität München, Germany (Prof. R. Vogel's group) [49]. Briefly, *L. lactis* NZ9000 (Δ*lmrA*), an *lmrA* deletion strain containing pNHlmrA, a plasmid that permits expression of His-tagged LmrA protein under control of the nisin system (NICE) was kindly provided by Driessen and van den Berg van Saparoea [50–52]. Cells were grown in M17 medium (Difco) supplemented with 0.5% (w/v) glucose and 5 ng/mL chloramphenicol. *Purification of His6-LmrA.* Histidine-tagged LmrA was purified using the protocol described before [50] with the following modifications: cells were grown at 30 °C to an OD 660 of 0.6–0.8. LmrA expression was induced by addition of 0.5 ng/mL Nisin A and cells were grown for further 90 min. Cells were harvested, washed with 50 mM HEPES–KOH (pH 7.0) and resuspended in the same buffer. Membrane vesicles were prepared via ultrasonic treatment on ice (10 s, cycle 0,5, amplitude 80%) for three times (with 6 cycles each) with 20 s intercooling on ice using a ultrasonic processor UP 200s (Hielscher Ultrasonics GmbH, Teltow, Germany) followed by a 10 s treatment with a homogenizer Miccra D-8 DS-20/PG (stage A). Cell debris and unbroken cells were removed at 13,000 g at 4 °C for 30 min. Membrane vesicles were collected using an ultra centrifuge (125,000 g, 1 h, 4 °C), washed twice in 50 mM HEPESKOH (pH 7.0) with 10% glycerol, centrifuged (280,000 g, 30 min, 4 °C), resuspended in the same buffer, frozen in liquid nitrogen and stored at −80 °C. Membrane lipids were solubilised as described [50] and mixed with Ni Sepharose 6 Fast Flow beads, (~25 μL of beads/mg of protein) which was pre-equilibrated in buffer A (50 mM Hepes–KOH (pH 8.0), 0.3 M NaCl, 10% (v/v) glycerol, and 0.05% (w/v) DDM) containing 40 mM imidazole. The suspension was incubated for 1 h at 4 °C, transferred to a centrifuge tube, centrifuged for 2 min at 1000 g, washed 5 times with 4 volumes of buffer A and protein was eluted with buffer B (pH 7.0), having the same composition as buffer A but containing 280 mM imidazole (all steps at 4 °C). The purified protein was used immediately for reconstitution in proteoliposomes or frozen in liquid nitrogen and stored at −80 °C.

2.2. Sample preparation

2.2.1. Lipid extraction from L. plantarum TMW 1.460

L. plantarum was used for the extraction of a natural lipid mixture. It has a LmrA transporter as well, but grows better than *L. lactis*, which thus results in a higher yield of lipids. The membrane lipids of *L. plantarum* TMW 1.460 were extracted and purified from the cell mass as described in [26] with some modifications. 10 L of modified MRS, pH 6.5 (per litre: 2 g meat extract, 10 g tryptic digest casein peptone, 4 g yeast extract, 1.8 g potassium dihydrogen phosphate, 5 g sodium acetate, 4 g diammonium hydrogen citrate, 88 g glucose, 0.1 g magnesium sulfate, 0.05 g manganous sulfate, 0.5 μg each of cobalamin, folic acid, niacin, pantothenic acid, pyridoxal, and thiamin) were inoculated over night with 50 mL culture of *L. plantarum TMW 1.460* and incubated for three days at 30 °C. The pH was adjusted every day to 6.0 with 5 M NaOH under non sterile conditions. The suspension was then centrifuged at 30 °C and 2500 g for 90 min, washed twice with 50 mM potassium phosphate, pH 7.0, and centrifuged for 15 min and 4000 g at 30 °C. After centrifugation, cells were frozen (−20 °C) and thawed, resuspended in 20 mM potassium phosphate, pH 7.0, at a concentration of 1 g/mL (wet weight) and incubated at 37 °C for 30 min with 4.2 mg/mL lysozyme and 0.01 mg/mL DNase. The following steps were carried out under N_2 atmosphere to avoid lipid oxidation. Chloroform and methanol were added at a volume ratio of 1:2 and the suspension was stirred overnight at 4 °C. Cell debris was removed by centrifugation at 2000 g for 10 min. The supernatant was added to chloroform and water (volume ratio 1:1:1) and the mixture

was stirred for 3 h at RT. Phase separation was permitted over night at 4 °C and the chloroform phase was evaporated in a rotary evaporator at 40 °C and redissolved in chloroform to a concentration of 0.1 g/mL. One aliquot of the mixture was given to 10 aliquots of ice cold acetone containing 5 mM β-mercatoethanol, stirred over night at 4 °C and centrifuged at 1000 g at RT. The supernatant, including neutral lipids (glycolipids) and a minor amount of other polar lipids (phosphatidylethanolamines and other non-choline containing phospholipids), was dried in a rotary evaporator. The pellet, including the phospholipids, was dried under nitrogen flow. Both fractions were resuspended in diethyl ether containing 5 mM β-mercatoethanol to a concentration of 0.1 g/15 mL, stirred for 1 h and centrifuged at 1000 g at RT. Pellets were dried under a nitrogen flow and supernatants in a rotary evaporator, and each fraction was checked for purity using TLC and stored at −20 °C. The major neutral lipid/glycolipid fraction (roughly 70% of the total mass of extracted lipids), which was soluble in acetone and diethylether, was chosen for the experiments only, as in the other fraction (containing charged phospholipids), impurities, such as remaining hydrophobic proteins, could not be excluded. Also, MLV could not be formed from the total natural lipid fraction (it emerged as too tightly packed).

2.2.2. Liposome preparation

Lipid and cholesterol stock solutions were prepared in chloroform. Laurdan was dissolved in chloroform at a concentration of 1 mmol/L, DMPC, DOPC, DMPC containing 10 mol% cholesterol, the natural lipid extract and vesicles containing the 1:2:1 molar ratio of DOPC, DPPC and Chol were prepared together with the fluorophore Laurdan (see below). After co-dissolving the respective lipids and fluorophore, the solvent chloroform was removed by a flow of nitrogen gas. Then the samples were dried under high vacuum pumping for several hours to completely remove the remaining solvent. The resulting dry film was then resuspended in 20 mM HEPES buffer, pH 7.2, vortexed and sonicated for 15 min in a bath-type sonicator (Bandelin SONOREX RK100SH). Large unilamellar vesicles were produced by five freeze–thaw cycles (freezing in liquid nitrogen and slow-thawing in a warm water bath) followed by 13 passages through two stacked Nucleopore polycarbonate membranes of 100 nm pore size in a mini-extruder. The samples were kept at 65 °C during the extrusion procedure. The final concentration of lipid vesicles in the samples used for the fluorescence measurements was 0.1 mg/mL. The final vesicle solution contained a 1:500 fluorophore to lipid mixture on a molecular basis. At these low fluorophore concentrations, no perturbation of the lipid bilayer structure is observed.

2.2.3. Proteoliposome preparation

Proteoliposomes of LmrA with DMPC, DOPC, DMPC+10 mol% cholesterol, the natural lipid extract and the model raft mixture DOPC:DPPC:Chol (1:2:1) were prepared by the successive detergent removal method [33]. Liposomes of the desired single- or multi-component lipid mixture were prepared by the sonication/freeze thaw cycles/extrusion method described above. The required amount of 1.5 mM detergent dodecyl maltoside (DDM) to destabilize the different liposomes was determined by light scattering measurements. Liposomes were destabilized by slow addition of the required amount of detergent DDM and stirring for 15 min at room temperature. For the reconstitution, the purified LmrA was mixed with DDM-destabilized liposomes in a 1:20 wt ratio and incubated for 30 min at room temperature under gentle stirring. The detergent was then removed by two successive extractions with SM2 biobeads. The polystyrene beads were thoroughly washed with methanol and water for 3 times before use. A wet weight of 80 mg biobeads/mL of liposomes was used to extract the detergent each time. The first extraction was performed at room temperature for 2 h and the second extraction at 4 °C for 16 h. Finally, proteoliposomes were collected by centrifugation (280,000 g, 30 min, 20 °C) and resuspended in 20 mM HEPES buffer, pH 7.2, at a final lipid concentration of 1 mg/mL.

2.3. Fluorescence spectroscopy

The fluorescence spectroscopic measurements were performed using a K2 multifrequency phase and modulation fluorometer with photon counting mode equipment (ISS Inc., Champaign, Ill). The operational principle of the multifrequency fluorometer has been described in detail elsewhere [34,35]. The temperature was controlled to ± 0.1 °C by a circulating water bath. Samples were pressurized by ethanol in a high pressure cell system made by the ISS company.

The phase state of the lipid membrane systems was determined by the Laurdan fluorescence technique. The emission spectrum of the environmentally sensitive fluorescence probe 6 dodecanoyl-2-dimethyl-aminonapthalene (Laurdan) was used to scrutinize the phase behavior of the lipid bilayer system. Laurdan is a naphthalene based amphiphilic molecule with an fluorescence excitation and emission spectra that are very sensitive to the polarity and to the dipolar dynamics of the environment [36,37]. The quantum yield of Laurdan is much higher in the membrane than in aqueous solution. When inserted into a membrane, Laurdan aligns its lauroyl tail with the lipid moiety and locates its naphthalene ring near the phospholipids glycerol backbone. Studies using phospholipid vesicles demonstrated that Laurdan is sensitive to the dynamics as well as the polarity of the surrounding membrane. Therefore, Laurdan can distinguish whether a membrane is in an ordered or fluid-like phase state [38]. When Laurdan is embedded in a lipid membrane, it exhibits a 50 nm red shift of the emission spectrum as the membrane changes from the gel to the liquid–crystalline phase. The spectral changes of the emission spectrum of Laurdan are generally quantified by the so-called generalized polarization function, which is defined as $GP=(I_B-I_R)/(I_B+I_R)$, where I_B and I_R are the fluorescence intensities at 440 nm (characteristic for an ordered, gel phase state environment) and 490 nm (characteristic for a fluid, liquid–crystalline lipid state), respectively [39]. Hence, *GP* values range from −1 to +1. In phase coexistence regions, the *GP* values exhibit values typical for fluid (liquid-disordered) and gel-type (liquid-ordered) domains. Hence the measured *GP* values of our system reflect the overall phase behavior and fluidity of the membrane as a function of temperature and pressure. The error bars represent standard errors from at least three different measurements always using new sample preparations.

2.4. CD spectroscopy

Stock solutions of purified LmrA were prepared in 50 mM HEPES–KOH, pH 7.0, 300 mM NaCl, 10% glycerol, 250 mM imidazole, pH 7.0, and 0.05% DDM. The stock solution was diluted to 5 μM with 20 mM HEPES buffer, pH 7.0, for the CD spectroscopic measurements. CD spectra were recorded in a cylindrical thermocell (0.01 cm path length) from 190 to 260 nm in 1 nm steps on a JASCO J-715 CD spectrometer (Easton, MD) under constant nitrogen flush. Each spectrum is an average of 20 scans taken with a scan rate of 20 nm per minute. An external water thermostat was used to control the temperature within ± 0.1 °C. Temperature-dependent CD scans were carried out from 30 to 70 °C by stepwise increase of 5 °C. Samples were equilibrated at each temperature for 15 min. CD data are expressed as the mean residual ellipticity (MRE) [θ] in degrees cm^2 $dmol^{-1}$. The proportions of the secondary structural content of the protein were determined using the CDNN software [40].

2.5. Atomic force microscopy (AFM)

For the AFM studies, a freshly prepared LmrA proteoliposome sample (lipid–protein ratio 50:1 wt/wt, $c_{(lipid)}=1$ mg/mL) was extruded at 40 °C using an Avanti Miniextruder (Avanti Polar Lipids, Alabaster, AL) with polycarbonate membranes of 100 nm pore size to yield large unilamellar vesicles. Supported lipid bilayers for the AFM measurements were produced by depositing 60 μL of the LmrA

proteoliposome solution together with 30 μL of buffer (20 mM HEPES, 10 mM $MgCl_2$, pH 7.2) on freshly cleaved mica and incubation in a wet chamber overnight at 37 °C for DMPC and DMPC/cholesterol membranes as well as 45 °C for the DOPC/DPPC/cholesterol membranes. After incubation, the sample was allowed to cool to room temperature, carefully rinsed with buffer and placed on the AFM stage.

Measurements were performed on a MultiMode scanning probe microscope with a NanoScope IIIa controller (Digital Instruments, Santa Barbara, CA) and usage of a J-Scanner (scan size 125 μm× 125 μm) at room temperature (depending on the system, between about 21 and 28 °C). Images were obtained by applying the Tapping Mode in liquid with oxide-sharpened silicon nitride probes (DNP-S, Veeco Instruments, Mannheim) mounted in a fluid cell (MTFML, Veeco Instruments, Mannheim). Tips with nominal force constants of 0.32 N/m were used at driving frequencies around 9 kHz and drive amplitudes between 200 and 400 mV corresponding to the softness of the sample. Height and phase images of sample regions were acquired with a resolution of 512×512 pixels and scan frequencies between 0.5 and 1.5 Hz. All measurements were carried out at room temperature. Images were processed by using the NanoScope software version 5.

3. Results and discussion

Before investigating the temperature and pressure dependent phase changes of the reconstituted proteoliposomal systems, we first studied the temperature stability of the protein itself and verified its reconstitution into the various lipid bilayer systems using CD spectroscopic and AFM measurements, respectively.

3.1. Secondary structure of LmrA as function of temperature

The LmrA transporter is a homodimer, each unit consisting of a 590 amino acids residue monomer containing 6 transmembrane helixes in the amino terminal hydrophobic domain, followed by a large hydrophilic domain with ATP binding site. In the functional unit of the LmrA-homodimer, there are four core domains consisting of two transmembrane domains (one from each monomer unit) and two nucleotide binding domains. The secondary structure and the dynamics of the membrane embedded domains of LmrA have been studied, recently [41–43]. It is reported that the reconstituted LmrA alone or in the presence of ADP consists of 35% α-helices, 24% β-sheets, 28% β-turns and 13% random structures [42]. Here we report the temperature dependent secondary structural changes of non-reconstituted LmrA in DDM micelles. Temperature-dependent CD data were taken from 30 to 70 °C at 5 °C intervals. In Fig. 1, selected CD traces are shown. All the spectra depict a similar shape consisting of a double minimum band at ~210 and ~222 nm, and one maximum between 192 and 194 nm, which is characteristic of α-helices. For all temperatures, the molar ellipticity value falls in the negative region between 210 and 225 nm, indicating the presence of β-sheet structures. The spectra were deconvoluted using the CDNN software and the percentage of individual secondary structure elements was determined. Generally, the overall shape of the CD spectra and hence the proportion of the secondary structural elements did not change markedly with increasing temperature. According to our analysis, non-reconstituted LmrA protein incorporated in the DDM micelles contains about 26% α-helices, 24% β-sheets, 17% β-turns and 33% random coil-like structures. Hence, compared to the membrane embedded environment, the α-helix and β-turn contents are slightly smaller. The disordered structures increase concomitantly in the micellar environment, whereas the β-sheet content does not seem to be largely affected by the lipid surroundings. Fig. 2 depicts the changes of all secondary structural elements of LmrA with increasing temperature. The protein seems to be very temperature stable as no significant changes in secondary structure elements occur even up to temperatures as high as 70 °C.

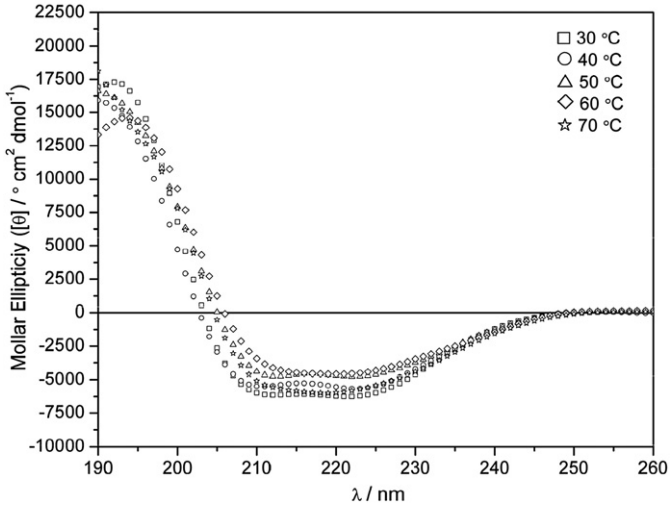

Fig. 1. CD spectrum of LmrA in DDM micelles as a function of temperature.

3.2. AFM measurements

Using AFM experiments, the previously described three model membrane systems – namely DMPC, DMPC/Chol, and DOPC/DPPC/Chol – were also examined. In all three lipid systems, one extensive lipid bilayer can be detected on the mica on which smaller areas of up to three additional lipid bilayers are located. In the LmrA reconstituted DMPC sample, up to three lipid bilayers can be identified (Fig. 3a). The first lipid bilayer with incorporated LmrA protein shows a thickness of ~6.2 nm (red arrows in the section analysis), the second ~6.0 nm and the third bilayer ~6.6 nm. The black areas in the figure are defects in the first lipid bilayer so that the underlying mica can be seen. A few vesicles (e.g., two on the lower right side), which had not fused on the mica surface, appear as big white spots. The LmrA protein is spread nearly homogeneously over the whole membrane (light brown small dots, black arrows in the section analysis), but there are also small domains without incorporated protein. Notably, the incorporation of the protein leads to a thickening (due to an increase of lipid conformational order and/or a decrease of the chain's tilt angle) of the membrane which is reflected in a height difference of about 1.8 nm (green arrows in the section analysis). The membrane domains without protein show a thickness of around 4.5 nm which would correspond to a pure ordered DMPC domains [44,45]. The extramembranous domains of the incorporated LmrA protein protruding from the bilayer vary in size from 0.7 nm to 6.7 nm with a median of 3.1 nm (histogram in Fig. 3a). This particle size distribution may be explained by the membrane topology of the LmrA protein [28,43]. The six membrane-spanning regions cause the N- and C-terminus of the protein being located at the same side of the membrane. The particles with a smaller height could be due to the membrane protruding part of 34 amino acids of the N-terminus and the loops (5–65 amino acids) connecting the transmembrane domains. On the other hand, the larger particle heights observed may represent the larger C-terminal hydrophilic nucleotide-binding domain (NBD, 278 amino acids). The particle size is probably also influenced by the orientation and dynamics of the membrane protruding parts with respect to the bilayer plane.

In the liposomes consisting of DMPC and 10 mol% cholesterol and being reconstituted with LmrA protein, up to four lipid bilayers can be seen (Fig. 3b). The thickness of the lipid bilayers are ~6.4 nm for the first (green arrows in the section analysis), ~6.3 nm for the second, ~6.4 nm for the third, and ~6.6 nm for the fourth lipid bilayer. Again,

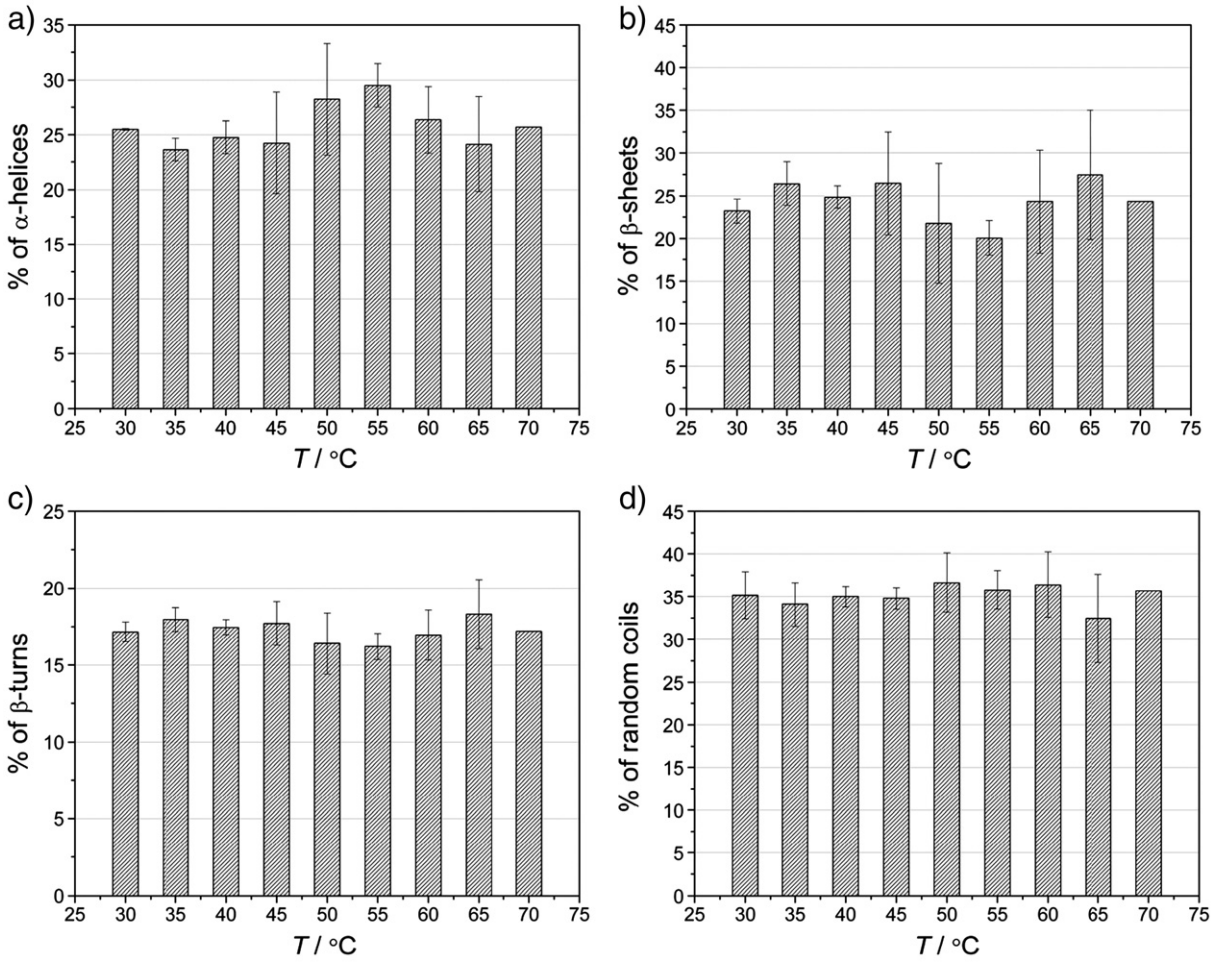

Fig. 2. Percentage of secondary structural elements as a function of temperature. (a) α-helics, (b) β-sheets, (c) β-turns, and (d) random coils.

the protein is spread nearly homogeneously over the whole membrane, but there are also domains without or less incorporated protein (dark brown region on the right side of the image). Similar to the DMPC membrane system, the incorporation of the protein leads to a thickening effect in the membrane which is reflected in a height difference of about 1.7 nm (red arrows in the section analysis). The membrane domains without protein show a thickness of around 4.7 nm, which is in agreement with the previously determined 4.5 nm for ordered DMPC domains. A size distribution between 1.3 nm and 6.6 nm with a median of 2.9 nm was detected for the membrane protruding parts of the LmrA protein being incorporated into DMPC/Chol membranes (histogram in Fig. 3b and black arrows in the section analysis).

For the proteoliposome consisting of the model raft mixture DOPC/DPPC/Chol (1:2:1), up to three bilayers are observed (Fig. 3c). In the protein-containing liquid-ordered (l_o) phase, the first lipid bilayer shows a thickness of ~7.0 nm (red arrows in the section analysis), the second of ~6.9 nm, and the third lipid bilayer of ~6.8 nm. The difference between the pure l_o- and l_d-phases is around 1.1 nm (green arrows in the section analysis). The bilayers with embedded LmrA exhibit a thickness of about 5.8 nm in the liquid-disordered (l_d) phase. As in the previous membrane systems, the LmrA protein is spread nearly homogeneously over the membrane. Interestingly, the LmrA protein is incorporated in both, the l_o and l_d domains. Again, the incorporation of the protein leads to a thickening effect of the membrane which is reflected in a height difference of about 1.7 nm (the membrane domains without protein show a thickness of around 5.2 nm in the l_o-phase and of around 4.1 nm in the l_d-phase). The membrane protruding parts of the incorporated LmrA protein exhibit a size between 0.7 nm and 6.4 nm with a median of 2.4 nm (histogram in Fig. 3c and black arrows in the section analysis).

3.3. Temperature- and pressure-dependent phase behavior of DMPC-LmrA lipid bilayers

The effect of temperature and pressure on the generalized polarization data of Laurdan labeled DMPC bilayers without and with incorporated LmrA are shown in Figs. 4a and b, respectively. The pure DMPC lipid bilayers exhibit a rather sharp gel-to-fluid (P_{β}'–L_{α}) phase transition around T_m=24 °C. Reconstitution of LmrA into DMPC bilayers induces a broad gel–fluid phase coexistence region with a markedly increased conformational order of the lipid acyl chains above the gel–fluid phase transition temperature of DMPC. Below T_m, LmrA only slightly disturbs the packing order and hence the *GP* values are slightly reduced, only.

Upon pressurization, the pressure-induced fluid-to-gel phase transition takes place around 70 MPa at 37 °C in pure DMPC (Fig. 4b), in good agreement with literature data [6,7]. The Clapeyron slope of the transition has been determined to be $dT/dp \approx 0.21$ °C/MPa [6]. Reconstitution of LmrA leads to an increasing overall conformational ordering of the membrane in the whole pressure range covered, i.e. from 1 to 200 MPa. The pressure dependent phase behavior does not change significantly upon the reconstitution of LmrA. Above 90 MPa, a plateau *GP* value is reached in both pure (*GP*=0.44) and reconstituted (*GP*=0.49) DMPC vesicles. All the graphs presented here comprise the average of three independent measurements.

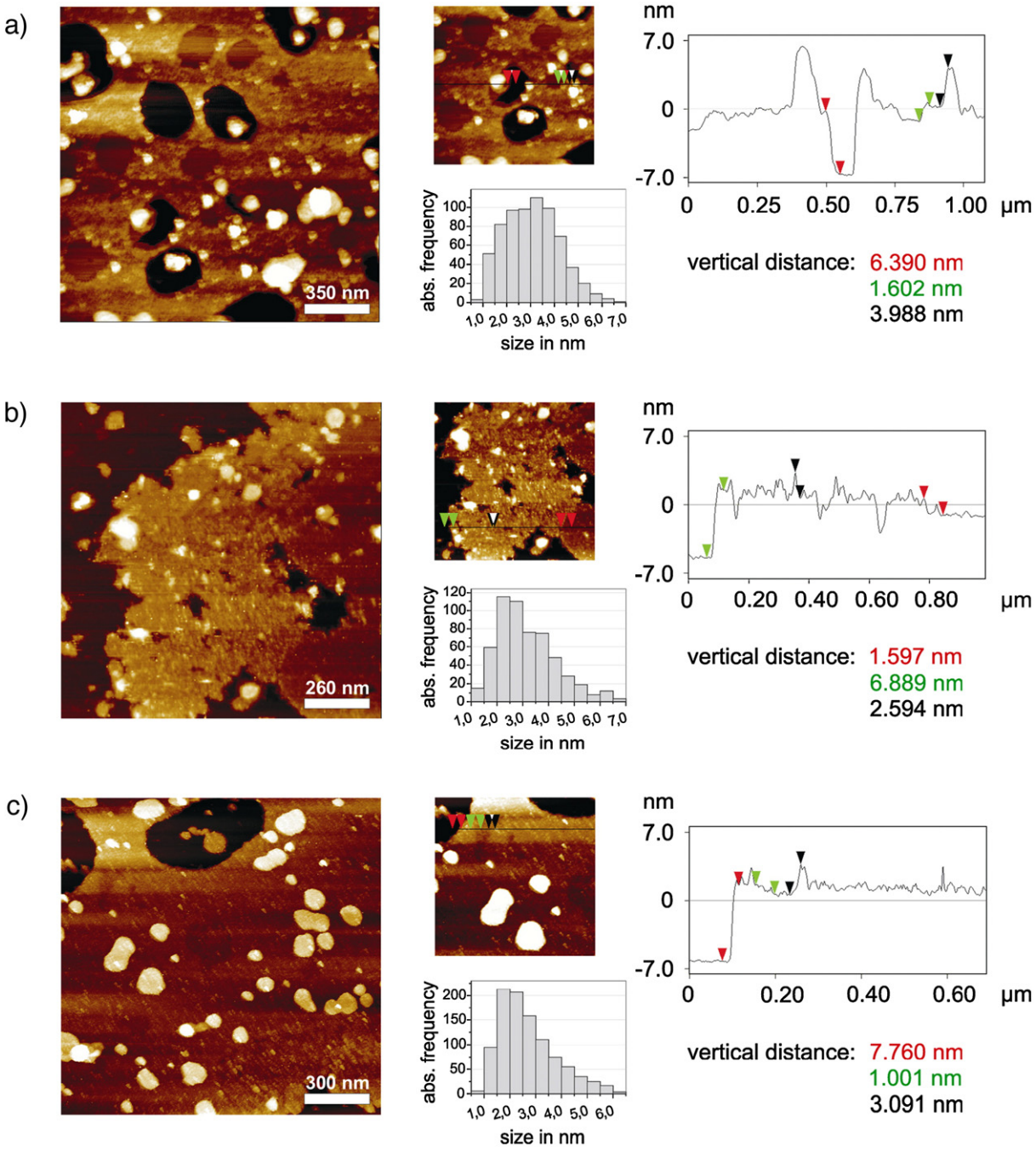

Fig. 3. AFM measurements of proteoliposomes with the transmembrane protein LmrA incorporated into lipid bilayers being composed of (a) DMPC, (b) DMPC/10 mol% cholesterol, and (c) DOPC/DPPC/Chol (1:2:1). On the left hand side, the whole scan area is shown with a vertical color scale from dark brown to white corresponding to an overall height of 15 nm, 25 nm, and 25 nm for A, B, and C, respectively. The concomitant section profiles of the AFM image are given on the right hand side. The horizontal black line in the middle figure is the localization of the section analysis shown on the right, indicating the vertical distances between pairs of arrows (black, green and red). The size distribution of the extra-membranous parts of the incorporated LmrA protein protruding from the bilayer is given in the concomitant histogram for each measurement.

3.4. Temperature- and pressure-dependent phase behavior of DOPC-LmrA lipid bilayers

The effect of temperature and pressure on the generalized polarization data of Laurdan labeled DOPC bilayer without and with incorporated LmrA are depicted in Figs. 5a and b, respectively. Due to the presence of two unsaturated acyl chain, the transition temperature of DOPC is about −20 °C [5,7]. Hence, throughout the measurement range (3 to 50 °C) the DOPC bilayers are in the liquid-disordered state, which is characterized by very low *GP* values (Fig. 5a). With increasing temperature, the fluidity of the acyl chains is still increasing as indicated by the further slight decrease in the *GP* value. Pure DOPC bilayers at 3.7 °C exhibit a *GP* value of 0.09, which is gradually reduced to −0.36 at 50 °C. Reconstitution of LmrA does not significantly change the average chain order parameter, still, there is a very small increase of *GP* value throughout the whole temperature range covered (Fig. 5b).

As revealed by the pressure dependent *GP* measurements at 37 °C, the mean order parameter steadily increases with increasing pressure, as seen in Fig. 5b. The *GP* value of pure DOPC bilayer at 0.1 MPa (1 bar) is −0.31, which linearly increases to 0.02 at 200 MPa. As in the case of

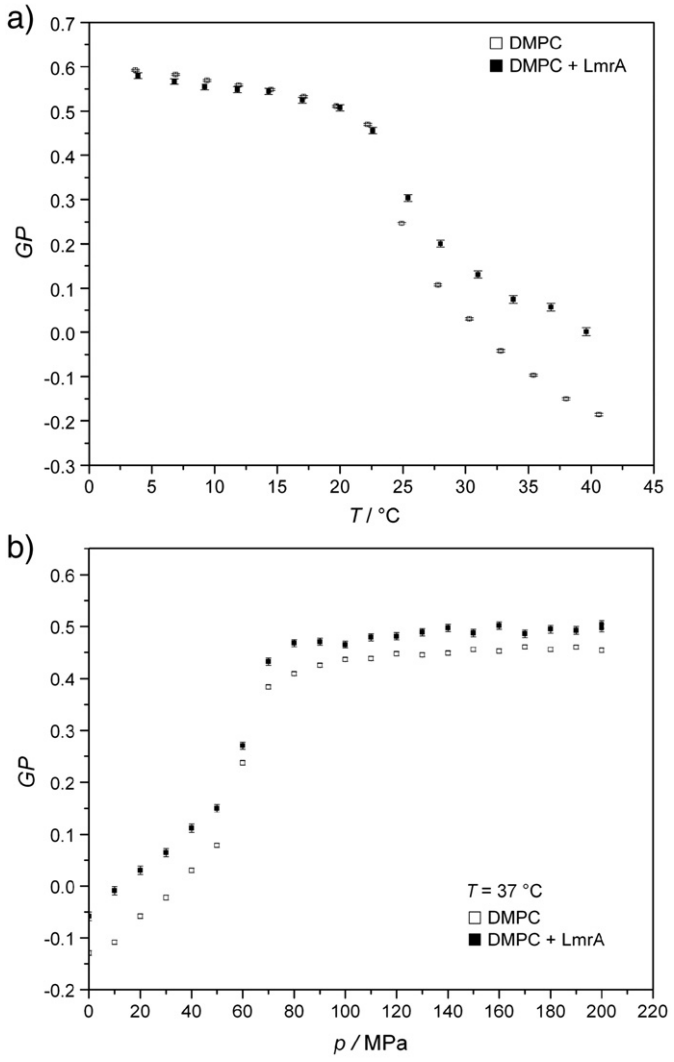

Fig. 4. (a) Temperature dependence of Laurdan *GP* values of DMPC vesicles without and with reconstituted LmrA (at 0.1 MPa). (b) Pressure dependence (at T=37 °C) of Laurdan *GP* values of DMPC vesicles without and with reconstituted of LmrA.

temperature dependent measurements, the reconstitution of LmrA into the DOPC bilayers does not lead to a marked change of the pressure dependent phase behavior of the DOPC bilayers. The mean order parameter of LmrA reconstituted into DOPC system is only slightly higher than that of the pure DOPC bilayer up to 120 MPa, and slightly reduced at higher pressures (>120 MPa) for T=37 °C. Obviously, different from fluid DMPC bilayers, incorporation of LmrA into DOPC does not lead to significant changes in the overall order parameter profile of this longer-chain fluid lipid bilayer system.

3.5. Temperature- and pressure-dependent phase behavior of DMPC/10 mol% cholesterol–LmrA lipid bilayers

As clearly seen from Fig. 6a, the incorporation of 10 mol% of cholesterol into pure DMPC lipid bilayers largely broadens the sharp gel-to-fluid ($P_{\beta'}/L_{\alpha}$) phase transition and significantly increases the chain order parameter in the fluid phase of the system, as evidenced by the increase of *GP* in the cholesterol containing lipid system compared to that of pure DMPC. Reconstitution of LmrA into the 10 mol% cholesterol containing DMPC bilayer leads to a further increase in the conformational order of the lipid acyl chains above the gel-to-fluid phase transition temperature of DMPC, and, similar to pure DMPC, leads to no significant changes in the packing order below T_m.

The effect of pressure on the generalized polarization data of Laurdan labeled cholesterol containing DMPC bilayers without and with embedded LmrA is shown in Fig. 6b. Upon pressurization, the pressure-induced fluid-to-gel phase transition takes place around 70 MPa at 37 °C, i.e., at a similar pressure as in the pure DMPC bilayer system. Reconstitution of LmrA leads to an overall increasing conformational order of the acyl chains in the entire pressure range studied (1 to 200 MPa). Hence, the pressure dependent phase behavior does not change markedly upon the reconstitution with LmrA. Plateau *GP* values of 0.54 in DMPC/10 mol% cholesterol and of 0.57 in the case of the LmrA containing bilayer system are reached around 90 MPa.

3.6. Temperature- and pressure-dependent phase behavior of the raft model membrane without and with incorporated LmrA

Fig. 7a depicts the temperature dependent *GP* values of the canonical raft mixture DOPC:DPPC:Chol (1:2:1). We have used this canonical model raft mixture using cholesterol as sterol, although cholesterol is not highly present in bacterial cells, because the structure and phase behavior of this heterogeneous lipid bilayer system has been studied in most detail [47]. Also, different sterols reveal minor differences in their ordering behavior, only [48], and

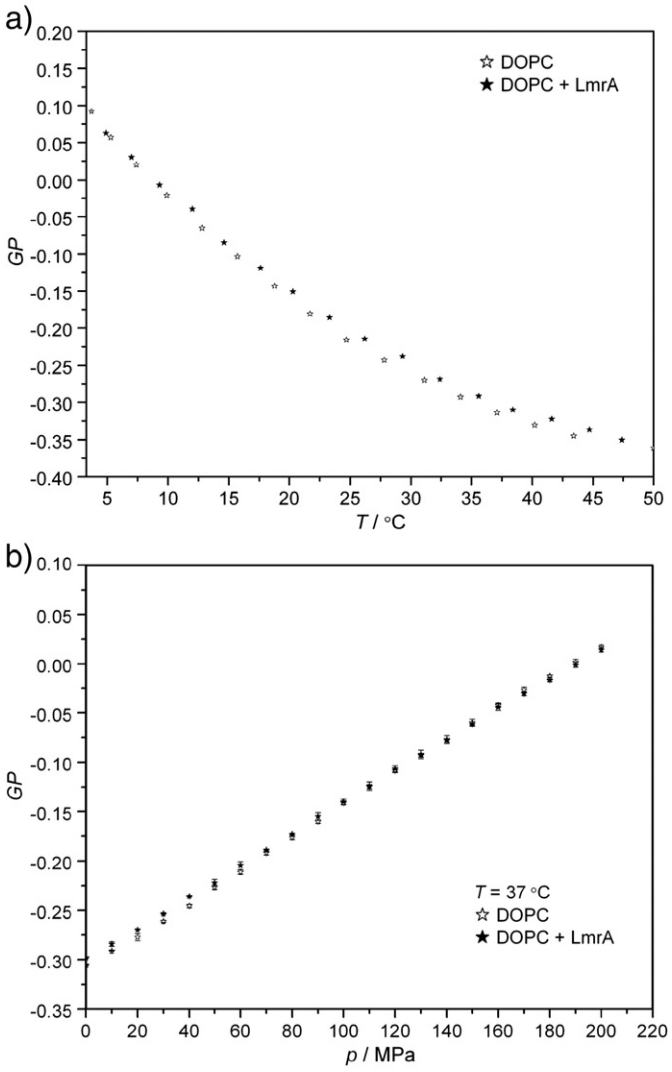

Fig. 5. (a) Temperature dependence of Laurdan *GP* values of DOPC vesicles without and with reconstituted LmrA (at 0.1 MPa). (b) Pressure dependence (at T=37 °C) of Laurdan *GP* values of DOPC vesicles without and with reconstituted of LmrA.

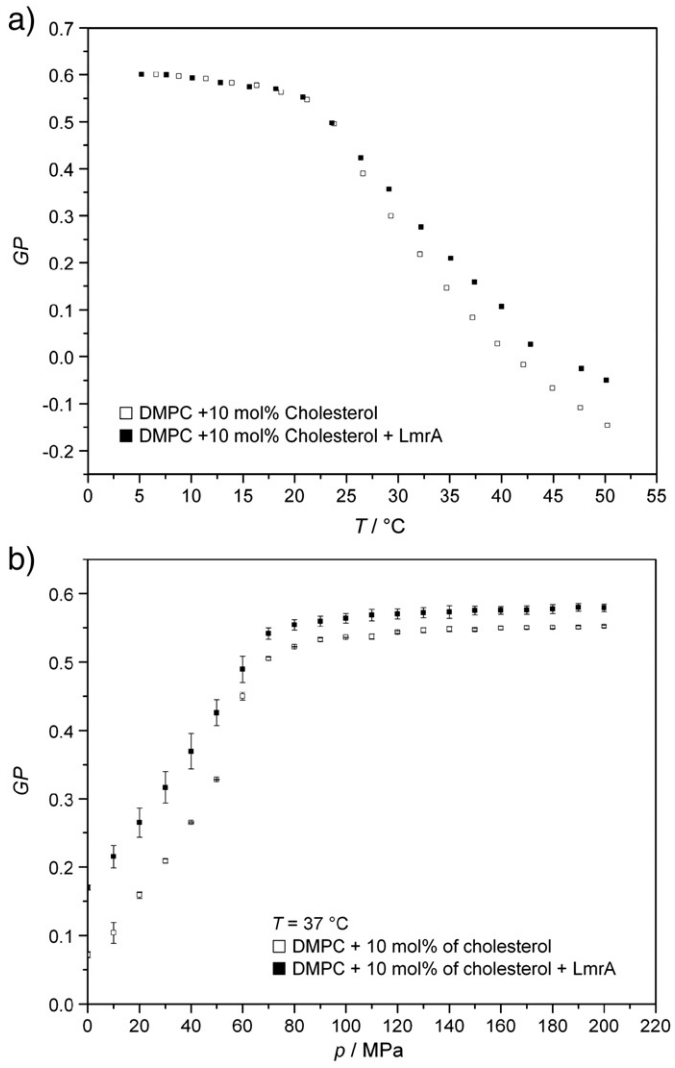

Fig. 6. (a) Temperature dependence of Laurdan *GP* values of lipid vesicles made of DMPC/10 mol% cholesterol without and with reconstituted LmrA (at 0.1 MPa). (b) Pressure dependence (at T=37 °C) of Laurdan *GP* values of vesicles made of DMPC/10 mol% cholesterol without and with reconstituted of LmrA.

similar transporters are known in eukariotic cells. The measurements were taken over a temperature range from 5 to 65 °C. This ternary lipid system exhibits a physiologically probably more relevant l_o and l_d domain coexistence region at ambient temperatures [46]. As can be clearly seen in Fig. 7a, the generalized polarization value gradually decreases with increasing temperature, with a sigmoidal kind of shape in the temperature interval between about 15 (*GP*=0.58) and 65 °C (*GP*=−0.05). This type of temperature dependent order parameter profile and phase behavior is consistent with that of other model raft systems, such as of POPC:SM:Chol [47]. In fact, such behavior of *GP*(T) is expected from Gibb's phase rule for three-component lipid mixtures, which is very different from, e.g., pure DMPC one-component lipid bilayer systems, which exhibit rather sharp gel-to-gel and gel-to-fluid phase transitions in the temperature range covered. By a more or less continuous increase of liquid-disordered domains, the fluidity and conformational disorder of the ternary lipid mixture gradually increases with increasing temperature, and *GP* values typical for pure fluid phases are reached at about 60 °C for DOPC:DPPC:Chol (1:2:1). No clear-cut value for the transition temperature to the overall fluid phase can be given owing to the continuous nature of the transition and hence *GP*(T) curve, however. Reconstitution of LmrA into the lipid system leads to a very small, but readily reproducible increase of *GP* in the lower temperature range of 5 to 30 °C. This was confirmed by the AFM measurements (see above). Above about 30 °C, LmrA incorporation has no effect on the orientational order of the acyl chains.

The effect of pressure on the generalized polarization data of the Laurdan labeled DOPC:DPPC:Chol model raft mixture is shown in Fig. 7b, which exhibits *GP* data at 40 °C as a function of pressure up to 200 MPa. In both, the pure and the LmrA reconstituted raft lipid system, the *GP* value increases steadily with increasing pressure and approaches plateau values of *GP* above about 160 MPa of 0.55 and 0.58, respectively, indicating that a rather ordered (probably an s_o+l_o) state is reached in this pressure regime. At much higher pressures, the transition to an all s_o phase could be envisaged. However, as the lipid mixture contains cholesterol and DPPC, which might not pack well against *cis*-unsaturated lipids, this could be prohibited. *GP* values up to 40 MPa in the reconstituted system are slightly smaller than those of the pure lipid system, and above 40 MPa, the *GP* values exhibit slightly higher values. Altogether, it is clearly seen that the reconstitution of LmrA into the model raft membrane does not drastically affect the overall temperature and pressure dependent phase behavior and conformational order of this heterogeneous membrane system.

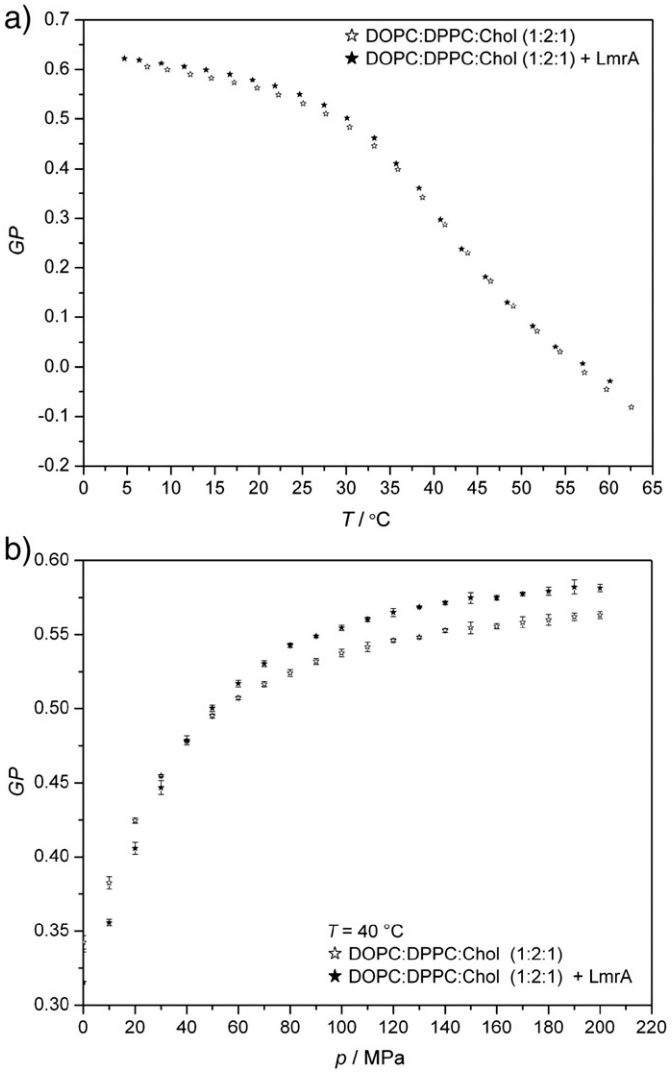

Fig. 7. (a) Temperature dependence of Laurdan *GP* values of vesicles made of the model raft lipid mixture DOPC/DPPC/Chol (1:2:1) without and with reconstituted LmrA (at 0.1 MPa). (b) Pressure dependence (at T=40 °C) of Laurdan *GP* values of vesicles of the same systems.

3.7. Temperature- and pressure-dependent phase behavior of the natural lipid system without and with incorporated LmrA

Lipids extracted from *L. plantarum* TMW 1.460 mainly contain phosphatidylglycerol along with diphosphatidylglycerol (cardiolipin). Other phospholipids detected in decreasing amounts include sphingomyelin, lyso-phosphatidylglycerol, diacylglycerol and free fatty acids. The effect of temperature and pressure on the generalized polarization data of the Laurdan labeled major, neutral/glycolipid fraction without and with incorporated LmrA are shown in Figs. 8a and b, respectively. Due to the complex nature of this natural lipid extract, no sharp phase transitions are observed, rather a continuous decrease of *GP* with increasing temperature is seen. Around 50 °C, a plateau *GP* value of ~0.2 is reached. This value represents a significantly higher order of the acyl chains compared to all model membrane systems studied at this temperature, indicating a rather compact packing of the lipid chains with high orientational order even at high temperatures. Remarkably, reconstitution of LmrA profoundly increases the acyl chain order of the membrane. The effect is strongest at temperatures higher than about 25 °C. Above 37 °C, the reconstituted lipid system reached a maximum *GP* value of 0.43.

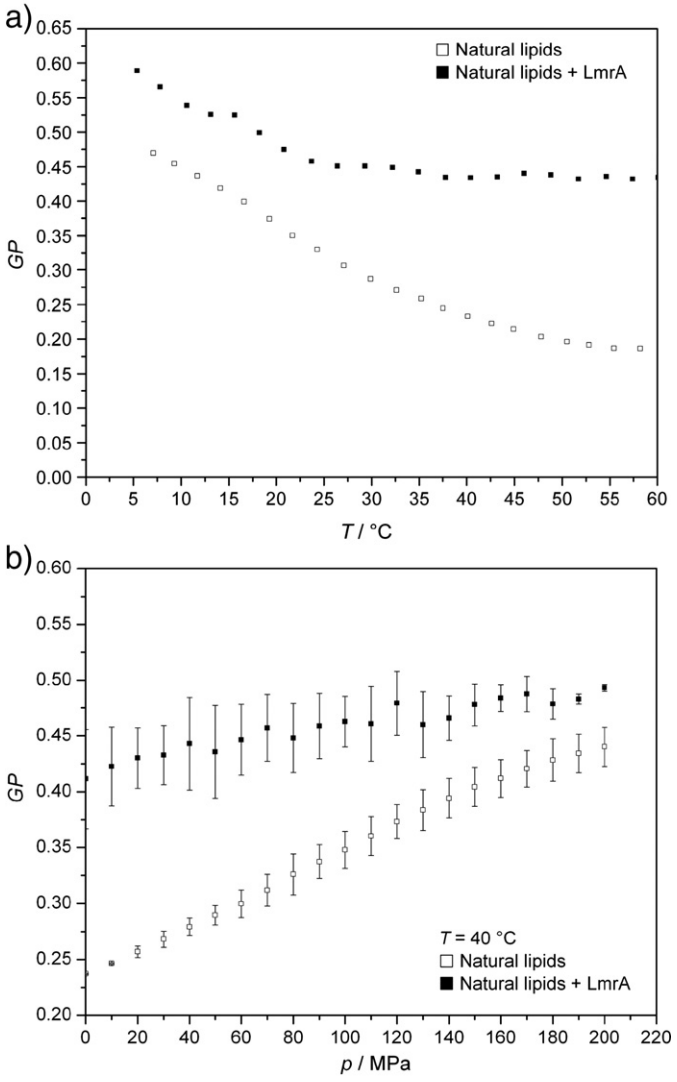

Fig. 8. (a) Temperature dependence of Laurdan *GP* values of vesicles made of the natural lipid extract from *Lactobacillus plantarum* without and with reconstituted LmrA (at 0.1 MPa). (b) Pressure dependence (at T=40 °C) of Laurdan *GP* values of vesicles made of the same systems.

Upon pressurization of the non-reconstituted natural membrane system, the overall conformational order of the membrane increases continuously in the whole pressure range covered, i.e., from 1 to 200 MPa. Over this pressure range, the *GP* value increases from 0.24 to 0.44. Reconstitution of LmrA into this natural lipid environment leads to an overall increase in the conformational order of the acyl chains throughout the whole pressure range. Notably, the reconstituted system is much less sensitive to environmental hydrostatic pressure changes. The *GP* value of the reconstituted system increases from 0.41 at ambient pressure to *GP*=0.49 at 200 MPa, only. The standard deviation of three separate readings was used for calculation of the error bars.

4. Discussion and conclusions

Before studying the temperature and pressure dependent changes upon reconstitution of LmrA into the various model membrane systems including membranes from natural lipid extracts, we first studied the temperature stability of the protein itself and verified its reconstitution into the various lipid bilayer systems. The temperature dependent secondary structure of the LmrA in DDM micelles was measured from 30 to 70 °C by CD spectroscopy. The average proportion of the secondary structures has been determined to be 26% α-helices, 24% β-sheets, 17% β-turns and 33% random coil conformations and does not change markedly with increasing temperature, indicating a high temperature stability even up to 70 °C, thus allowing us to carry out measurements in various lipid bilayer systems even up to such high temperatures.

To reveal proper reconstitution and the partitioning of the LmrA in the various model membrane systems, tapping mode AFM experiments were carried out. The height images clearly indicate that the reconstitution process was successful and that the incorporation of the transmembrane protein LmrA leads to an ordering effect of fluid lipid bilayers, which is reflected in an increase in membrane thickness of about 1.7 nm. Interestingly, the LmrA shows no phase preference in the canonical raft mixture, i.e., the protein is located in both, the l_o- and l_d-domains of the DOPC/DPPC/Chol (1:2:1) mixture. The size distribution of the LmrA protein parts protruding from the membrane's surface may be explained by the different sizes of the 34 amino acid N-terminal domain, the loops and the large hydrophilic C-terminal ATP-binding domain.

In a second step, the effect of LmrA reconstitution on the temperature and pressure dependent conformation and phase behavior of various model membrane systems was studied, finally aiming at correlating these structural properties with the functional state of LmrA embedded in these various lipid matrices upon pressurization.

Both the sterol cholesterol and the transmembrane protein LmrA exhibit similar effects on fluid DMPC. They broaden the gel-fluid transition and increase the overall conformation order of the lipid acyl chains of the DMPC (C_{14}) bilayers above its main phase transition temperature. Reconstitution of LmrA into cholesterol containing DMPC bilayers further increases the ordering of the fluid lipid acyl chains, as evidenced by an increase of *GP* by an additional 0.1 units.

Reconstitution of LmrA into fluid DOPC ($C_{18:1,cis}$) bilayers did hardly increase the conformational order of its longer acyl chains; a very small increase of the *GP* value was observed throughout the whole temperature range covered, only. The corresponding hydrophobic thicknesses of the DMPC and DOPC bilayers are 2.2 and 2.7 nm, respectively. Owing to the larger ordering effect of LmrA on DMPC bilayers, one might conclude that a significant hydrophobic mismatch is present between fluid DMPC and the LmrA protein's hydrophobic transmembrane segment, which does not seem to be the case for the thicker DOPC bilayer.

Reconstitution of LmrA into the canonical model raft mixture DOPC:DPPC:Chol (1:2:1) leads to a very small, but readily reproducible

increase of *GP* in the lower temperature range from 5 to 30 °C, only, whereas above 30 °C the LmrA has no effect on the orientational order of the acyl chains. This, again, may be due to the absence of a significant hydrophobic mismatch between the membrane-spanning part of LmrA and the lipid membrane. The AFM data reveal that the protein is accommodated in both, the l_o and l_d domains of this heterogeneous model membrane. Please note that in this three-component mixture, some lipid sorting is feasible to prevent lipid mismatch in both phases.

Remarkably, reconstitution of LmrA into the major, neutral/glycolipid fraction of the natural lipid extract leads to a drastic increase of the overall conformational order of the acyl chains in the whole temperature range covered, with *GP* values as high as 0.47 even up to 60 °C. This might be due to a lack of hydrophobic matching between the lipid bilayer made up of this particular lipid fraction (lacking also all the other protein components, which are expected to increase the membrane order upon incorporation into the lipid bilayer) and the hydrophobic part of the membrane spanning protein.

As has been shown by many studies on phospholipid bilayer model systems, by increasing pressure by only a few hundred bars (ten MPa), the acyl-chain conformational order drastically increases and a more or less broad gel-fluid coexistence region as well as several pressure-induced gel-phases may be induced at higher pressures [6,7,12,47], which might hinder conformational transitions associated with the membrane protein's function. In case of the pure and cholesterol (10 mol%) containing DMPC bilayer systems, upon pressurization the pressure-induced fluid-to-gel phase transition takes place around 70 MPa at 37 °C ($dT/dp \approx 0.21$ °C/MPa). Above 90 MPa, both systems are rather insensitive to further pressure change and a plateau *GP* value is reached. The mean order parameter of the fluid-like cis-unsaturated DOPC bilayer linearly increases with increasing pressure at a constant temperature of 37 °C. However, the *GP* value exhibited even at pressures as high as 200 MPa is less ($GP \approx 0.0$) than the *GP* values of the other model and natural membrane systems exhibited at ambient pressure (0.1 MPa), a consequence of the disordering effect of the two cis-double bonds in DOPC. In case of the raft model membrane system DOPC:DPPC:Chol (1:2:1), the *GP* value increases steadily with increasing pressure up to 50 MPa and thereafter it's rather insensitive to pressure. At ambient pressure, the raft mixture exhibits a *GP* value of 0.34 and reaches 0.56 at 200 MPa. This small change ($\Delta GP = 0.22$) in the *GP* value indicates that the system already exists in a relatively ordered conformational state throughout the pressure range covered. Remarkably, the neutral/glycolipid lipid extract is much less sensitive to pressure, and exhibits a *GP* value of 0.24 at 0.1 MPa and 0.44 at 200 MPa. This indicates that this system exists in a relatively ordered state throughout the whole pressure range.

Reconstitution of LmrA into the pure and cholesterol containing DMPC system leads to an increase in the overall conformational order of the membrane in the whole pressure range covered (1 to 200 MPa) at 37 °C, but the pressure dependent phase behavior does not change markedly upon the reconstitution of LmrA. A different scenario is observed for DOPC bilayers. The mean order parameter of LmrA reconstituted into DOPC remains essentially unchanged. It is only slightly higher than that of the pure DOPC bilayer up to 120 MPa and it is slightly reduced at higher pressures (>120 MPa) at 37 °C. In the case of the raft model system, only domain-averaged conformational properties of the membrane are detected. Up to 40 MPa, the system exhibits a slightly smaller acyl chain order compared to that of the pure lipid system, and above 40 MPa, *GP* values indicate a slightly higher conformational order. Reconstitution of LmrA into the natural lipid extract leads to a large increase in the overall conformational order of the acyl chains at all pressures. As the order parameter of the pure lipid system is already rather high ($GP = 0.41$ at 0.1 MPa), the reconstituted system is rather insensitive to environmental hydrostatic pressure changes ($GP = 0.49$ at 200 MPa).

To conclude, the data show that the effect of the LmrA membrane protein on the conformation and phase state of the lipid matrix depends on the fluidity and hydrophobic matching conditions of the lipid system. This effect is most pronounced for fluid DMPC and DMPC with low cholesterol levels, but minor for longer-chain phospholipids such as DOPC and model raft mixtures such as DOPC/DPPC/Chol (1:2:1). The latter have the additional advantage of allowing lipid sorting to avoid substantial hydrophobic mismatch. The most drastic effect was observed for the major, neutral/glycolipid natural lipid mixture. In this case, the impact of LmrA incorporation on the increase of the conformational order of the lipid membrane was most pronounced. As a consequence, the membrane reaches a mechanical stability which makes it very insensitive to application of pressures as high as 200 MPa.

Finally, the data may be correlated with the functional properties of LmrA in these various lipid environments and upon application of high hydrostatic pressure, and compared with those on other membrane protein systems. Teichert showed that a sharp pressure-induced fluid-to-gel phase transition without the possibility for lipid sorting, such as for DMPC bilayers, has a drastic inhibitory effect on the LmrA activity [49]. Otherwise, an overall fluid-like membrane phase over the whole pressure-range covered, with suitable hydrophobic matching, such as for DOPC, prevents the membrane protein from total high pressure inactivation even up to 200 MPa. It cannot be ruled out, however, that the higher pressure stability is due to the larger fluidity and hence increased compressibility of the DOPC bilayer. Also the systems exhibiting thicker membranes with higher lipid order parameters, such as DMPC/10 mol% cholesterol and the model raft mixture, exhibit significant pressure stabilities at high pressure. For the natural lipid mixture, a more-phasic pressure dependence of the enzyme activity was found (probably connected to the observed significant changes of membrane structure upon protein incorporation), with some remaining activity at high pressures [49]. What seems to be clear, however, is that an efficient packing with optimal lipid adjustment to prevent (also pressure-induced) hydrophobic mismatch might be a particular prerequisite for the homodimer formation and hence function of LmrA.

Recently, we also investigated the influence of hydrostatic pressure on the activity of Na^+,K^+-ATPase enriched in the plasma membrane from rabbit kidney [17]. The data show that the activity of Na^+,K^+-ATPase is inhibited reversibly by pressures below 200 MPa, and an apparent activation volume of the pressure-induced inhibition reaction of $\Delta V^{\neq} = 47.1$ mL mol^{-1} was determined. At higher pressures, exceeding 200 MPa, the enzyme is inactivated irreversibly, in agreement with data of Chong et al. [16] and de Smedt et al. [18] who concluded that the decrease in the fluidity of the membrane caused by increased pressure might hinder the conformational changes that accompany the reaction steps, and thus decrease the rate of the overall reaction. Kato et al. suggested that high pressures up to 200 MPa might as well lead to a dissociation of the subunits of the Na^+,K^+-ATPase [21]. To be able to explore the effect of the lipid matrix on the enzyme activity, the enzyme was also reconstituted into various lipid bilayer systems of different chain length, conformation, phase state and heterogeneity including model raft mixtures [17]. Similar to the enzyme activity in the natural plasma membrane, high hydrostatic pressures lead to a decline of the activity of the enzyme reconstituted into various lipid bilayer systems. Interestingly, in the low-pressure region, around 10 MPa, a significant increase of the activity was observed for the enzyme reconstituted into DMPC and DOPC bilayers. The enzyme activity decreased to zero around 2 kbar for these reconstituted systems measured. A different scenario was observed for the effect of pressure on the enzyme activity in a model raft mixture. The coexistence of liquid-ordered and liquid-disordered domains with the possibility of lipid sorting in this lipid mixture lead to a reduced pressure sensitivity in the medium pressure range. A similar stabilizing effect has been observed for LmrA [47]. Pressures

above about 220 MPa irreversibly changed the protein conformation of Na^+,K^+-ATPase, however, probably due to dissociation and partial unfolding of its subunits.

The effect of pressure was also measured on the HorA activity of *L. plantarum*. Changes were determined in the membrane composition of *L. plantarum* induced by different growth temperatures and their effect on the pressure inactivation, and a temperature–pressure phase diagram was constructed for the *L. plantarum* membranes that could be correlated with the respective kinetics of high pressure inactivation. Upon pressure-induced transitions to rigid (e.g., gel-like) membrane structures, i.e. at pressures around 50–150 MPa for temperatures between 20 and 37 °C, similar to the LmrA system studied here, fast inactivation of HorA was observed [20].

Recently, pressure has also been found to be of interest to study perturbations of signalling events, such as ToxR–ToxR interaction and phospholipase activation by G-proteins [53–56]. Scarlata revealed perturbations of phospholipase PLβ-Gβγ association caused by the Gα(GDP) subunit in the membranous context that where not observable by atmospheric association measurements [55]. PLCβ membrane binding was stable throughout the 0.1–200 MPa range, Gβγ only at high concentrations, whereas Gα(GDP) dissociated from membranes above 100 MPa. Pressure experiments on ion channels at high pressure are still scarce as well. They revealed that high pressures below 100 MPa affect the kinetics of gating (generally, a retardation is observed due to a positive activation volume, possibly owing to a conformational change following a change in dipole moment) but not the conductance of the channel [56].

The study of high-pressure effects on membrane proteins and in particular on ion channels and signalling processes is still in its infancy, but there are sufficient published experiments now to encourage further work in this growing area. What is already clear is that the membrane physical–chemical effects markedly influence the lipid–protein interaction, activity and pressure stability of the membrane protein. It seems also to be clear that the specific nature of the membrane protein (e.g., oligomeric assembly, a required dimerization reaction, etc.) plays a significant role in its pressure-dependent activity and stability as well.

Acknowledgements

Financial support from the Deutsche Forschungsgemeinschaft (DFG) and the Fonds der Chemischen Industrie is gratefully acknowledged.

References

[1] P. Yeagle (Ed.), The Structure of Biological Membranes, CRC Press, Boca Raton, 1992.
[2] R.B. Gennis (Ed.), Biomembranes: Molecular Structure and Function, Springer-Verlag, New York, 1989.
[3] O.G. Mouritsen, Life as a Matter of Fat, Springer-Verlag, Berlin Heidelberg, Germany, 2003.
[4] G.S. Attard, R.H. Templer, W.S. Smith, A.N. Hunt, S. Jachowski, Modulation of CTP: phosphocholine cytidylyltransferase by membrane curvature elastic stress, Proc. Natl. Acad. Sci. U. S. A. 97 (2000) 9032–9036.
[5] G. Cevc (Ed.), Phospholipids Handbook, Marcel Dekker, Inc, New York, 1993.
[6] R. Winter, Synchrotron X-ray and neutron small-angle scattering of lyotropic lipid mesophases, model biomembranes and proteins in solution at high pressure, Biochim. Biophys. Acta 1595 (2002) 160–184.
[7] R. Winter, W. Dzwolak, Temperature–pressure configurational landscape of lipid bilayers and proteins, Cell. Mol. Biol. 50 (2004) 397–417.
[8] C. Nicolini, J. Baranski, S. Schlummer, J. Palomo, M.L. Burgues, M. Kahms, J. Kuhlmann, S. Sanchez, E. Gratton, H. Waldmann, R. Winter, Visualizing association of N-ras in lipid microdomains: influence of domain structure and interfacial adsorption, J. Am. Chem. Soc. 128 (2006) 192–201.
[9] F. Meersman, L. Smeller, K. Heremans, Protein stability and dynamics in the pressure–temperature plane, Biochim. Biophys. Acta 1764 (2006) 346–354.
[10] K. Heremans, Pressure effects on biochemical systems, In: H. Kelm (Ed.), High Pressure Chemistry, Reidel Publishing Company, Dordrecht, Netherlands, 1978, pp. 467–487.
[11] C. Nicolini, J. Kraineva, M. Khurana, N. Periasamy, S.S. Funari, R. Winter, Temperature and pressure effects on structural and conformational properties of POPC/SM/Cholesterol model raft mixtures — a FT-IR, SAXS, DSC, PPC and Laurdan fluorescence spectroscopy study, Biochim. Biophys. Acta 1758 (2006) 248–258.
[12] J. Eisenblätter, R. Winter, Pressure effects on the structure and phase behavior of DMPC-Gramicidin lipid bilayers — a synchrotron SAXS and ^{2}H-NMR spectroscopy study, Biophys. J. 90 (2006) 956–966.
[13] I. Daniel, P. Oger, R. Winter, Origins of life and biochemistry under high pressure conditions, Chem. Soc. Rev. 35 (2006) 858–875.
[14] J.L. Silva, D. Foguel, C.A. Royer, Pressure provides new insights into protein folding, dynamics and structure, Trends Biochem. Sci. 26 (2001) 612–618.
[15] D. Foguel, C.R. Robinson, P.C. de Sousa, J.L. Silva, A.S. Robinson, Hydrostatic pressure rescues native protein from aggregates, Biotechnol. Bioeng. 63 (1999) 552–558.
[16] P.L.G. Chong, P.A.G. Fortes, D.A. Jameson, Mechanisms of inhibition of (Na,K)-ATPase by hydrostatic pressure studied with fluorescent probes, J. Biol. Chem. 260 (1985) 14484–14490.
[17] E. Powalska, S. Janosch, E. Kinne-Saffran, R.K.H. Kinne, C.F.L. Fontes, J.A. Mignaco, R. Winter, Fluorescence spectroscopic studies of pressure effects on Na^+, K^+-ATPase reconstituted into phospholipid bilayers and model raft mixtures, Biochemistry 46 (2007) 1672–1683.
[18] H. de Smedt, R. Borghgraef, F. Ceuterick, K. Heremans, Pressure effects on lipid–protein interactions in (Na^+, K^+)-ATPase, Biochim. Biophys. Acta 556 (1979) 479–489.
[19] J.T. Penniston, High hydrostatic pressure and enzymic activity: inhibition of multimeric enzymes by dissociation, Arch. Biochem. Biophys. 142 (1971) 322–332.
[20] H.M. Ulmer, H. Herberhold, S. Fahsel, M.G. Gänzle, R. Winter, R.F. Vogel, Effects of pressure-induced membrane phase transitions on inactivation of HorA, an ATP-dependent multidrug resistance transporter, in *Lactobacillus plantarum*, Appl. Environ. Microbiol. 68 (2002) 1088–1095.
[21] M. Kato, R. Hayashi, T. Tsuda, K. Taniguchi, High pressure-induced changes of biological membrane. Study on the membrane-bound Na^+/K^+-ATPase as a model system, Eur. J. Biochem. 269 (2002) 110–118.
[22] M.O. Souza, T.B. Creczynski-Pasa, H.M. Scofano, P. Gräber, J.A. Mignaco, High hydrostatic pressure perturbs the interactions between CF_0F_1 subunits and induces a dual effect on activity, Int. J. Biochem. Cell Biol. 36 (2004) 920–930.
[23] R. Winter (Ed.), High Pressure Bioscience and Biotechnology II, Springer-Verlag, Heidelberg, Germany, 2003.
[24] M.C. Roberts, Tetracycline resistance determinants: mechanisms of action, regulation of expression, genetic mobility, and distribution, FEMS Microbiol. Rev. 19 (1996) 1–24.
[25] P. Mazurkiewicz, A.J. Driessen, W.N. Konings, Energetics of wild-type and mutant multidrug resistance secondary transporter LmrP of *Lactococcus lactis*, Biochim. Biophys. Acta 1658 (2004) 252–261.
[26] A. Margolles, M. Putman, H.W. van Veen, W.N. Konings, The purified and functionally reconstituted multidrug transporter LmrA of *Lactococcus lactis* mediates the transbilayer movement of specific fluorescent phospholipids, Biochemistry 38 (1999) 16298–16306.
[27] K. Sakamoto, A. Margolles, H.W. van Veen, W.N. Konings, Hop resistance in the beer spoilage bacterium *Lactobacillus brevis* is mediated by the ATP-binding cassette multidrug transporter HorA, J. Bacteriol. 183 (2001) 5371–5375.
[28] H.W. van Veen, K. Venema, H. Bolhuis, I. Oussenko, J. Kok, B. Poolman, A.J. Driessen, W.N. Konings, Multidrug resistance mediated by a bacterial homolog of the human multidrug transporter MDR1, Proc. Natl. Acad. Sci. U. S. A. 93 (1996) 10668–10672.
[29] H. Bolhuis, H.W. van Veen, D. Molenaar, B. Poolman, A.J. Driessen, W.N. Konings, Multidrug resistance in *Lactococcus lactis*: evidence for ATP-dependent drug extrusion from the inner leaflet of the cytoplasmic membrane, EMBO J. 15 (1996) 4239–4245.
[30] H. Bolhuis, D. Molenaar, G. Poelarends, H.W. van Veen, B. Poolman, A.J. Driessen, W.N. Konings, Proton motive force-driven and ATP-dependent drug extrusion systems in multidrug-resistant *Lactococcus lactis*, J. Bacteriol. 176 (1994) 6957–6964.
[31] C.F. Higgins, ABC transporters: from microorganisms to man, Annu. Rev. Cell Biol. 8 (1992) 67–113.
[32] H.W. van Veen, A. Margolles, M. Müller, C.F. Higgins, W.N. Konings, The homodimeric ATP-binding cassette transporter LmrA mediates multidrug transport by an alternating two-site (two-cylinder engine) mechanism, EMBO J. 19 (2000) 2503–2514.
[33] J.L. Rigaud, B. Pitard, D. Levy, Reconstitution of membrane proteins into liposomes: application to energy-transducing membrane proteins, Biochim. Biophys. Acta 1231 (1995) 223–246.
[34] R.D. Spencer, G. Weber, Influence of Brownian rotations and energy transfer upon the measurements of fluorescence lifetimes, J. Chem. Phys. 52 (1970) 1654–1663.
[35] T. Parasassi, F. Conti, E. Gratton, Time-resolved fluorescence emission spectra of Laurdan in phospholipid vesicles by multifrequency phase and modulation fluorometry, Cell Mol. Biol. 32 (1986) 103–108.
[36] W. Yu, P.T.C. So, T. French, E. Gratton, Fluorescence generalized polarization of cell membranes: a two-photon scanning microscopy approach, Biophys. J. 70 (1996) 626–636.
[37] E. Gratton, M.M. Limkeman, A continuously variable frequency cross-correlation phase fluorometer with picosecond resolution, Biophys. J. 44 (1983) 315–324.
[38] T. Parasassi, G. De Stasio, G. Ravagnan, R.M. Rusch, E. Gratton, Quantitation of lipid phases in phospholipid vesicles by the generalized polarization of Laurdan fluorescence, Biophys. J. 60 (1991) 179–189.
[39] T. Parasassi, G. De Stasio, A. d'Ubaldo, E. Gratton, Phase fluctuation in phospholipid membranes revealed by Laurdan fluorescence, Biophys. J. 57 (1990) 1179–1186.

[40] G. Böhm, R. Muhr, R. Jaenicke, Quantitative analysis of protein far UV circular dichroism spectra by neural networks, Protein Eng. 5 (1992) 191–195.
[41] V. Grimard, C. Vigano, A. Margolles, R. Wattiez, H.W. van Veen, W.N. Konings, J.M. Ruysschaert, E. Goormaghtigh, Structure and dynamics of the membrane-embedded domain of LmrA investigated by coupling polarized ATR-FTIR spectroscopy and $^{1}H/^{2}H$ exchange, Biochemistry 40 (2001) 11876–11886.
[42] C. Vigano, A. Margolles, H.W. van Veen, W.N. Konings, J.M. Ruysschaert, Secondary and tertiary structure changes of reconstituted LmrA induced by nucleotide binding or hydrolysis. A Fourier transform attenuated total reflection infrared spectroscopy and tryptophan fluorescence quenching analysis, J. Biol. Chem. 275 (2000) 10962–10967.
[43] A. Siarheyeva, J.J. Lopez, I. Lehner, U.A. Hellmich, H.W. van Veen, C. Glaubitz, Probing the molecular dynamics of the ABC multidrug transporter LmrA by deuterium solid-state nuclear magnetic resonance, Biochemistry 46 (2007) 3075–3083.
[44] Z.V. Feng, T.A. Spurlin, A.A. Gewirth, Direct visualization of asymmetric behavior in supported lipid bilayers at the gel–fluid phase transition, Biophys. J. 88 (2005) 2154–2164.
[45] J.A. Wieland, A.A. Gewirth, D.E. Leckband, Single-molecule measurements of the impact of lipid phase behavior on anchor strengths, J. Phys. Chem. B 109 (2005) 5985–5993.
[46] S.L. Veatch, S.L. Keller, Separation of liquid phases in giant vesicles of ternary mixtures of phospholipids and cholesterol, Biophys. J. 85 (2003) 3074–3083.
[47] N. Periasamy, R. Winter, The effects of temperature, pressure and peptide incorporation on ternary model raft mixtures — a Laurdan fluorescence spectroscopy study, Biochim. Biophys. Acta 1764 (2006) 398–404.
[48] C. Bernsdorff, R. Winter, Differential properties of the sterols cholesterol, ergosterol, β-sitosterol, *trans*-7-dehydrocholesterol, stigmasterol and lanosterol on DPPC bilayer order, J. Phys. Chem. B 107 (2003) 10658–10664.
[49] H. Teichert, Behaviour of membrane transport proteins under high hydrostatic pressure, Dissertation, Technische Universität München, 2008.
[50] H.B. van den Berg van Saparoea, J. Lubelski, R. van Merkerk, P.S. Mazurkiewicz, A.J. Driessen, Biochemistry 44 (2005) 16931–16938.
[51] I. Mierau, M. Kleerebezem, Appl. Microbiol. Biotechnol. 68 (2005) 705–717.
[52] O. Gajic, G. Buist, M. Kojic, L. Topisirovic, O.P. Kuipers, J. Kok, J. Biol. Chem. 278 (2003) 34291–34298.
[53] F. Abe, C. Kato, K. Horikoshi, Pressure-regulated metabolism in microorganisms, Trends Microbiol. 447 (1999) 447–453.
[54] F. Abe, Exploration of the effects of high hydrostatic pressure on microbial growth, physiology and survival: perspectives from piezophysiology, Biosci. Biotechnol. Biochem. 71 (2007) 2347–2357.
[55] S. Scarlata, Determination of the activation volume of PLCβ by Gβγ-subunits through the use of high hydrostatic pressure, Biophys. J. 88 (2005) 2867–2874.
[56] A.G. Macdonald, Experiments on ion channels at high pressure, Biochim. Biophys. Acta 1595 (2002) 387–389.